Available online at www.sciencedirect.com
ScienceDirect
Journal of Solid State Chemistry 180 (2007) 3008–3018
JOURNAL OF SOLID STATE CHEMISTRY
www.elsevier.com/locate/jssc

Designed synthesis of cobalt and its alloys by polyol process

R.J. Joseyphus[a], T. Matsumoto[b], H. Takahashi[a], D. Kodama[a], K. Tohji[a], B. Jeyadevan[a,*]

[a]*Graduate School of Environmental Studies, Tohoku University, Aramaki Aoba-ku, Sendai 980-8579, Japan*
[b]*Division of Materials Control, Institute of Multidisciplinary Research for Advanced Materials, Tohoku University, Sendai 980-8577, Japan*

Received 21 May 2007; received in revised form 10 July 2007; accepted 23 July 2007
Available online 10 August 2007

Abstract

The role of polyol, precursor and reaction promoting agents in the synthesis of metal and alloy nanoparticles using polyol process has been investigated by analyzing the reaction steps involved in the synthesis of cobalt in Co ion-polyol-[OH^-] ion system in detail. The reducing potential of polyols and the easiness with which any metal salt can react to form reducible complexes has been evaluated using the orbital molecular theory and the results were experimentally verified. The reduction limit of polyol and their extension using reaction promoting agents such as [OH^-] ions is also explained. The reduction of cobalt is preceded by various reaction stages of complex/compound formation, which has been fully identified. Furthermore, the reducing form of cobalt has been identified as either cobalt alkoxide or cobalt hydroxide. The results confirmed that the complex forming reactions that take place prior to the formation of the precursor, which finally get reduced to metal, play a decisive role in determining the physical properties of the nanoparticles. The approach can be extended to reduce any metals or alloys using polyol process.

Keywords: Polyol process; Cobalt nanoparticles; Cobalt complex; Reduction

1. Introduction

The synthesis of metal particles in polyols has been a subject of active research [1–3] in recent years. However, due to limited knowledge on the process itself, most of the work up to now has been confined to the synthesis of precious metals and their alloys [4–7] besides for a few exceptions [8–10]. Although the physical properties such as size, shape and crystal structure [11–13] of the particles have been controlled by manipulating the synthesis conditions that influence the nucleation and growth steps, no attempts have been made to fully understand the reaction mechanism that would lay the foundation for the synthesis of transition metal alloys and other functional alloy nanoparticles. As a consequence, particles with novel properties have been realized only through trial and error basis by carrying out large number of experiments varying all the experimental parameters randomly. Also, secondary reducing agents such as hydrazine or heterogeneous nucleating agents like Pt, Ru have to be used along with the polyols to accomplish enhanced reduction [14–16]. In some cases, the mechanism for the formation of metal nanoparticles proposed by the researchers has been found to be controversial. For example, the formation of Fe particles in polyols is claimed to be by disproportionation reaction and the role of polyol is said to be limited to solvent and not as a reducing agent [17]. But our recent studies have indicated that the polyols do have a strong role to play in reducing Fe at temperatures as low as 120 °C and also the properties of the iron particles depended on the type of polyol along with other experimental parameters such as reaction temperature and [OH^-] ion concentration [18]. The control of reaction condition could be utilized to obtain either Fe or Fe-oxides with various morphologies from Fe-alkoxides [19]. Hence the reducibility by polyol process and the ways to enhance the reduction has to be understood inorder to extend the process to synthesis any metal or alloy. Thus we provide insight information on the entire reactions that take place during the formation of cobalt metal in polyols from both theoretical and experimental aspects, considering the

*Corresponding author.
E-mail address: jeya@mail.kankyo.tohoku.ac.jp (B. Jeyadevan).

0022-4596/$ - see front matter © 2007 Elsevier Inc. All rights reserved.
doi:10.1016/j.jssc.2007.07.024

reactions undergone both by the reactants and polyols, to choose the reducibility of any metal in polyol.

Larcher and Patrice [20] presented a theoretical approach based on the estimation of the Gibbs free energy of the metal-polyol system to determine the reducing ability of oxides and hydroxides to obtain their respective metal particles. They studied the effect of type of polyol and starting material in the reduction of various metal ions and discussed their reducibility. However, it should be noted that this analysis will only provide us with the information about the possibility of any metal ion being reduced and will not provide any clue for the selection of metal salts or the parameters influencing the reduction of the same. Furthermore, the experimental observations have proved that the calculations are not consistent enough as some of the oxides and hydroxides with negative Gibbs free energy were not reduced. This anomalous behavior was explained on the basis of the formation of intermediate compound/complexes, which possess higher Gibbs free energy than the starting material. On the other hand, when the synthesis of cobalt metal or other cobalt based compound using polyol is considered, the emphasis has been on obtaining the end products of metal alone or metal oxides/alkoxides and not on the reaction scheme leading to the formation of the above [21–24]. Thus, an understanding of the reaction scheme during the reduction of metal ions in polyol is necessary to design the process for the synthesis of metals and alloys. Consequently, this may lead to the establishment of a generalized scheme for the reduction of metal ions in polyol. Hence, a detailed study has been undertaken to understand the influence of the type of reducing agent (polyol), type of metal salts, additives such as [OH^-], and reaction temperature to determine the rate determining steps involved prior to the formation of metal nanoparticles taking cobalt-[OH^-]-polyol system.

2. Experimental

In a typical experiment, either cobalt acetate tetrahydrate [$Co(OAc)_2 \cdot 4H_2O$] or cobalt chloride hexahydrate [$CoCl_2 \cdot 6H_2O$] of molar concentration 0.01 M was introduced directly into 100 mL of ethylene glycol (EG) or trimethylene glycol (TMEG) at room temperature (RT). Then, the metal salts-polyol system was heated at a rate of 15 °C/min to the boiling point of the polyol under constant mechanical stirring. For reactions involving [OH^-] ions, NaOH of 0.1 M is introduced along with the metal precursors at RT. The solution was sampled out for UV–visible spectroscopic studies at various reaction temperatures and duration. The selection of cobalt ion for this study was based on the fact that they enable the formation of various metal complexes and could function as a model element to extract information that will be useful to understand the behavior of other metals in polyol. Furthermore, the cobalt complexes formed prior to the generation of the solid precipitate are associated with color changes in the visible region. The formation of the complexes has been monitored by UV–visible spectroscopy, which is a useful tool employed to study the nanoparticle formation in noble metals and alloys [25,26] and also the reaction processes in aqueous systems.

The precipitates formed at various temperatures in polyols are also sampled out, centrifuged, washed in alcohol and dried for crystal phase and morphology analysis using X-ray diffractometer (XRD) (Rigaku) with a Cu target and a scanning electron microscope (SEM) (Hitachi S-4100). The morphology and electron diffraction patterns were also analyzed using a transmission electron microscope (TEM) (Hitachi HF2000). The UV–visible spectrum is recorded in a Hitachi UV–visible spectrometer by loading the sample in a quartz cell. The samples were scanned in the wavelength range of 300–800 nm with a scan speed of 2 nm/s in 1 nm step. The Fourier transform infrared spectrum (FTIR) is recorded in a Thermo Nicolet FTIR spectrometer (Avatar 360) fitted with a Duroscope in the scan range 800–4000 cm^{-1}. The theoretical estimation of the reaction rate of metal salts, and the reduction potential of polyols were determined from the *ab initio* calculations using Gaussian 98 [27] performed on a Compaq Alpha XP1000 computer. All geometrical optimizations were carried out by using the HF/LanL2MB basis set [28] to reduce calculation time and make them applicable to large molecules. The stability of the Hartree-Fock wave function was tested using stable option [29]. During *ab initio* calculations, all internal coordinates were optimized by means of the Berny algorithm, and convergence was tested against the criteria for the maximum force component, root-mean-square force, maximum displacement component, and root-mean-square displacement.

3. Results and discussion

For a given metal salt, the properties of nanoparticles such as size and its distribution, crystal structure, etc. synthesized by reducing the metal ions in polyol depends on the reaction rate of the process, which is a function of various experimental parameters described by the equation given below [30]

$$r = f(P_{\text{redox}}, M_{\text{conc.}}, H_{\text{conc.}}, T_{\text{reac.}}), \quad (1')$$

where $P_{\text{redox.}}$; the reduction potential of polyol, $M_{\text{conc.}}$; the metal ion concentration, $H_{\text{conc.}}$; the concentration of hydroxyl ions and $T_{\text{reac.}}$; the reaction temperature.

When the $P_{\text{redox.}}$ of the polyol is high, the metal ions are reduced rapidly forming an avalanche of nuclei consuming a large portion of the metal species and the particle diameter is consequently small due to the limited supply of metal ions for growth. Furthermore, the reaction rate is enhanced when the $H_{\text{conc.}}$ in metal ion—polyol system is increased. The concentration of hydroxyl ions [OH^-] necessary for the reduction of metal ions in polyol is also a function of the type of polyol. Highly reducing polyols need lesser amounts of [OH^-] to synthesize particles of comparable diameters [13]. The presence of [OH^-] in the

metal ion-polyol system is believed to act as a catalyst in accelerating the formation of precursor complexes. The effects of temperature ($T_{reac.}$) and molar concentration ($M_{conc.}$) on metal forming reaction in polyol are independent of other factors such as the type of metal salts, polyol and additives and the outcome could be predicted to a reasonable extent. Thus, we shall focus our discussions to the influence of experimental parameters like metal salts, additives and polyols on the reaction steps involved in polyol process.

3.1. Effect of metal salts

The synthesis of cobalt metal particles by polyol process is realized only with specific metal salts in polyols, which undergoes the next step of complex formation. In an octahedral and tetrahedral cobalt (II) complex, the transitions $^4T_{1g}(P) \leftarrow {}^4T_{1g}$ and $^4T_1(P) \leftarrow {}^4A_2$, respectively, can be observed in the visible region. In cobalt–chloride complexes, the absorption peaks at 575 nm corresponds to CoX_2Cl_2 where X represents pyridine, quinoline and alcohols whereas complex of the type $CoXCl_3^-$ or $CoCl_4^-$ could be identified from the absorption peak at 595 nm [31,32]. Similar behavior can be expected for cobalt acetate. The absorption at wavelengths 489 and 520 nm are characteristics of $[Co(H_2O)_6]^{2+}$ octahedral complex [31]. The absorption peak at 575 nm correspond to $CoX_2(L)_2$ (where X and L are EG and OAc here, respectively) as in the case of chloride systems, whereas other types of complexes like CoX_4Cl_2 show absorption around 525–540 nm and $CoXCl_3^-$ shows primary peak position at 595 nm [32]. Fig. 1 shows the UV–visible spectrum of cobalt (II) acetate tetrahydrate (continuous line) and cobalt chloride (broken line) in EG at a reaction temperature of 200 °C for various reaction times in the absence of [OH^-] ions. The UV–visible spectra at RT and 200 °C were similar for both the cobalt salts exhibiting absorption lines at wavelengths 489 and 520 nm. However, the spectrum of cobalt acetate began to vary with reaction duration exhibiting additional absorption lines at wavelengths 462 and 575 nm. The absorption peak intensity at 575 nm increases when the reaction duration is increased from 5 to 10 min whereas the lower wavelength absorption intensity decreases suggesting the transformation of acetates to complex of the type $CoX_2(OAc)_2$. However, in the case of cobalt chloride hexahydrate, the absorption spectra does not change significantly even after 1 h at 200 °C. This indicates that cobalt ion derived from cobalt acetate easily forms complexes compared to cobalt chloride. The chloride anion coordinates with the cation whose chemical bond is comparatively stable [23] and hence it is possible for the cobalt derived from acetates to form a complex more easily than chlorides. For example, the formation of $CoX_2(OAc)_2$ complex is a necessary condition for the reaction to proceed to form Co metals.

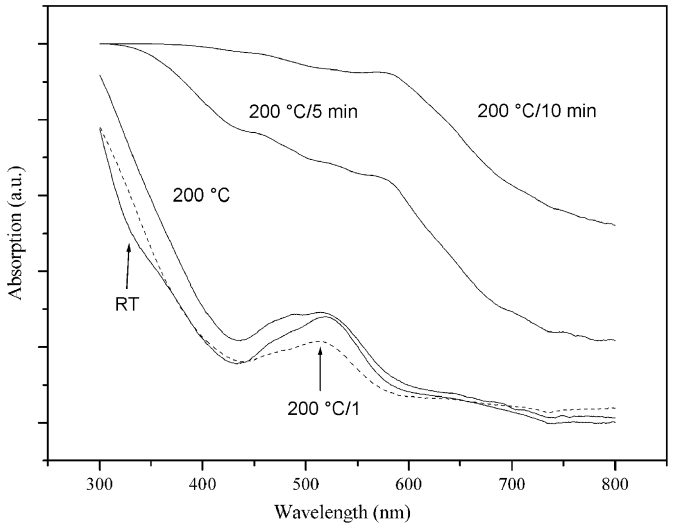

Fig. 1. The UV–visible spectrum of cobalt (II) acetate tetrahydrate in EG at various temperatures and reaction duration. The dotted line shows the UV–visible spectra of cobalt chloride hexahydrate in EG.

Besides the experimental evidence, we made an attempt to understand the behavior of these salts using molecular orbital theory, which also suggested that cobalt acetate transforms faster than cobalt chloride. On comparing the cobalt acetate with cobalt chloride, the values from molecular orbital calculations are given in Table 1. When we consider the values of cobalt acetate and cobalt chloride, it could be inferred from the table that the alpha occupied value for cobalt acetate is −8.716 eV whereas for cobalt chloride it is −11.878 eV that is lower than that for cobalt acetate. Similarly the other values of alpha and beta virtual and occupied of cobalt acetate are higher than chloride. Alpha represents the energy where orbital is at, without overlap of molecular orbital and beta corresponds to the overlap integral. The higher occupied and virtual alpha and beta values of cobalt acetate than their corresponding value for cobalt chloride, implies a faster reaction process for cobalt acetate in polyols (longer time taken for the formation of reducible form). From the experimental and theoretical considerations, we believe that the formation of reducible forms of metal complexes is the prime criteria and it is achieved rapidly when the metal salt is cobalt acetate. Hence, the synthesis of cobalt particles using cobalt acetate and chloride was attempted in the presence of [OH^-] ions.

3.2. Effect of hydroxyl ions

In polyols, the reduction of metals is accompanied by the dehydration and oxidation of the polyol. Thus the polyols are found to take part in the reaction process through the

Table 1
The result of the molecular orbital calculation for cobalt acetate and cobalt chloride. (unit: eV)

	Alpha occupied	Alpha virtual	Beta occupied	Beta virtual
$Co(OAc)_2$	−8.716	2.470	−8.800	2.731
$CoCl_2$	−11.878	0.942	−11.383	−2.177

equation mentioned below [1]:

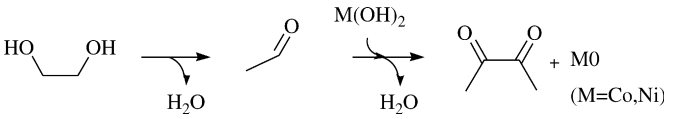

(1)

In the above equation, EG dehydrates to acetaldehyde followed by the formation of diacetyl [33]. It is believed that the [OH^-] ions help in the acceleration of the reaction through the enhancement in the formation of acetaldehyde. However there are no convincing reports on the enhancement in acetaldehyde. Hence, in order to verify the presence of acetaldehyde, and also to understand the role of [OH^-] ions in the reduction reaction, we performed 2,4 dinitrophenyl hydrazine test which is an indicator test for trace amount of carbonyls [34,35]. Here, the presence of a carbonyl is detected by the formation of 2,4 dinitrophenyl hydrazone on reacting the test solution of 2,4 dinitrophenyl hydrazine with acetaldehyde according to the following equation:

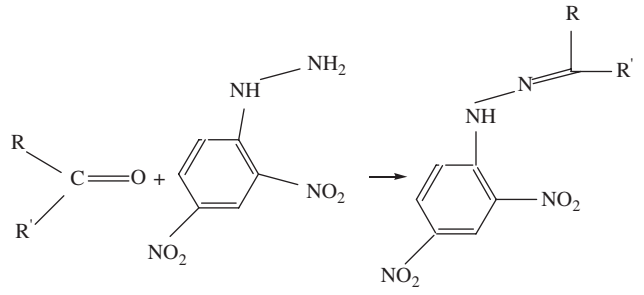

Carbonyl 2, 4 Dinitrophenyl hydrazine 2, 4 Dinitrophenyl hydrazone

(2)

The test solution was prepared by adding 20 ml of ethanol with 0.5 mM of 2,4 dinitrophenyl hydrazine and 2 drops of concentrated HCl. A positive test is detected by the formation of yellow or orange precipitate, whose presence is detected by appearance of absorption peaks in the UV–visible spectrum at 435 [36] and 358 nm [37]. We performed the experiments by directing the vapor from the EG at boiling point into the test solution of 2,4 dinitrophenyl hydrazine. The presence of acetaldehyde in the vapor of EG was confirmed as shown in Fig. 2. Thus, we carried out the above test in the presence of high concentration of [OH^-] and confirmed the enhancement in the peak intensity corresponding to acetaldehyde as shown in Fig. 2(c). Similar test was performed on EG solution heated to boiling temperature in the presence and absence of [OH^-] ions. However, the absorption peak indicating the presence of acetaldehyde was absent in either case that may be due to the lower boiling point of acetaldehyde (21 °C), which escapes out of the system. The confirmation of acetaldehyde from FTIR analysis is difficult for the same reason. Similar analysis was carried out using TMEG instead of EG and positive results were obtained. On the other hand, an attempt was made to study the influence of [OH^-] on the reduction reaction by analyzing the vapor generated during the reduction of cobalt ion for the presence

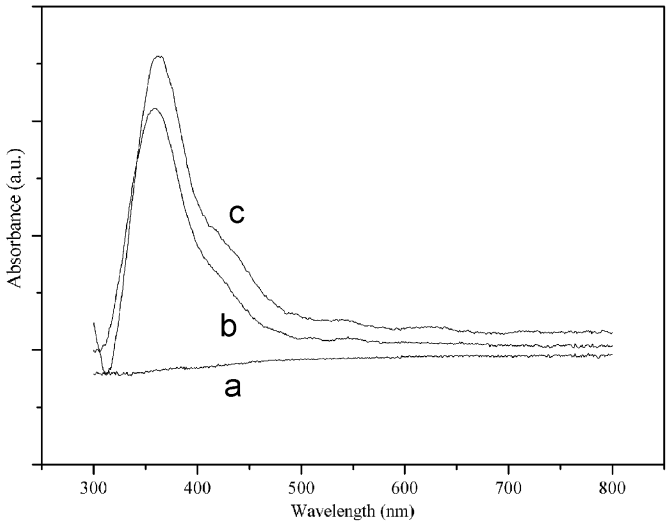

Fig. 2. The UV–visible spectrum of (a) EG solution, and vapors of EG (b) without [OH^-] and (c) with [OH^-] introduced into 2,4 dinitrophenyl hydrazine test solution. The absorption peaks indicate a positive test for acetaldehyde through the formation of 2,4 dinitrophenyl hydrozones.

of diacetyl by using FTIR. However, we were not successful due to insufficient concentration of diacetyl. Thus, the enhancement in the formation of acetaldehyde, which subsequently gets oxidized, may also help in the formation of hardly reducible metals such as Fe from ferrous ions. Fig. 3 illustrates the experimentally verified potential limit of polyol process in reducing various metal elements studied up to now. In this figure, the standard reduction potential (E°) of ions for reduction from and to various oxidation states in aqueous solutions at 25 °C is represented [38,39]. A higher standard reduction potential value represents easy formation of metals from their corresponding oxidation states. Although, the standard reduction potential of various ions in aqueous solution is compared at RT due to non-availability of sufficient data in polyols, the oxidation potentials of the polyols are lower than the reduction potential of metals at lower temperatures. However, the oxidation potential of polyol at higher temperatures, often at the boiling temperature of the polyol, reduces than that of the reduction potential of the metal as in the case of EG [40]. Hence the figure is an illustrative description of the reducing ability of polyols for various metal ions. The thick horizontal line in the figure represents the experimentally derived reduction potential limit of –0.403 V derived from the reduction of Cd by using polyol process. The dotted horizontal line represents the extension of the above limit to –0.447 V by introducing [OH^-] ions. This was demonstrated by the synthesis of pure Fe particles using EG–OH^- mixture, which was considered impossible [18]. In some cases like Mn, although the E^o value for reduction of Mn from 3^+ oxidation state is more than the other reducible ions, Mn could not be reduced in polyols. This is due to the fact that the standard potential for the Mn^{3+} to Mn^{2+} transition is positive whereas Mn^{3+} or Mn^{2+} to Mn^0 is more negative than the reduction potential limit of polyol. In contrast to

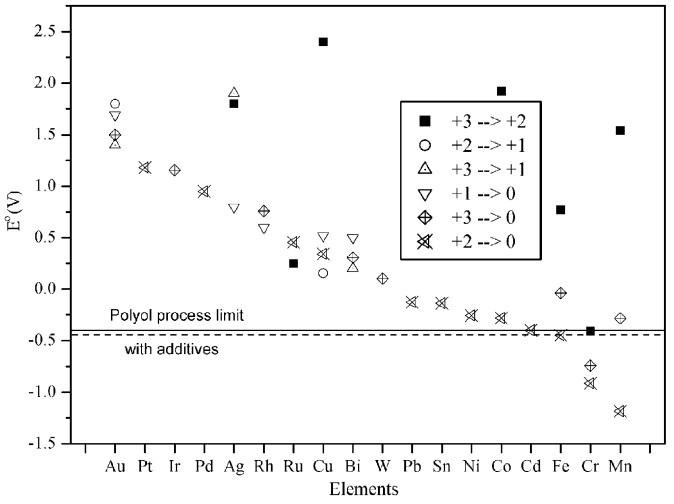

Fig. 3. The standard reduction potential of reduction from various oxidation states for various metal ions in aqueous solution at room temperature (from Refs. [38,39]) and the experimental reduction limit by polyol process.

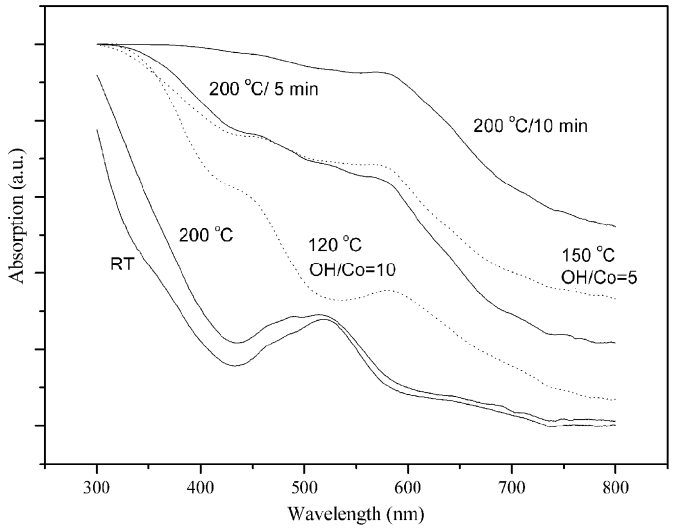

Fig. 4. The UV–visible spectrum of cobalt acetate tetrahydrate with (dotted line) and without [OH^-] (continuous line) in EG at various temperatures.

Mn, the reduction of Co^{2+} is more favored than Co^{3+} to obtain metallic Co.

Although the enhanced reaction rate with [OH^-] ions is observed in polyol process, the [OH^-] ions may also play a role in decreasing the reaction rate by forming metal hydroxide compounds that are not easily reduced, as observed in Pt system using H_2 as the reducing agent [41]. Here, the decrease in reaction rate is explained on the basis of the formation of less reducing complexes like $PtCl(OH)(H_2O)_2^-$ rather than $Pt(OH)_2$. Therefore, it is important to monitor the changes occurring in the system in the presence and absence of [OH^-] ions to confirm if the cobalt forms a complex or hydroxide. Hence, the effect of [OH^-] on the complex forming reactions in EG at various temperatures is monitored using UV–visible spectra. Fig. 4 shows the UV–visible spectra of $Co(OAc)_2$—EG and $Co(OAc)_2$—EG—[OH^-] systems at various reaction temperatures. The absorption spectrum of the solution in $Co(OAc)_2$—EG system at 200 °C for 5 min was different from that obtained at RT. However the absorption spectra at 150 °C in $Co(OAc)_2$—EG—[OH^-] system, for a [OH^-]/Co ratio of 5 resembles that of $Co(OAc)_2$—EG system reacted at 200 °C for 5 min. When the [OH^-]/Co ratio is increased further to 10, the absorption peaks appear even at 120 °C. The complex formed at high temperatures is tetrahedral $CoX_2(OAc)_2$ (where X is EG here) as observed in chloride system [32], which shows absorption at 575 nm. The XRD patterns of the intermediate precipitates obtained without [OH^-] ions was poorly crystalline while the one prepared with [OH^-] ions was well crystalline as shown in Fig. 5 (a) and (b), respectively. The XRD peaks for the precipitate obtained in the presence of [OH^-] ion is similar to the reported alkoxide [22,24] as seen from the main peak near 10° [22]. Since the cobalt alkoxides has the layered structure with turbostatic disorder and the interlayer spacings are occupied by the alkyl chains of the diol

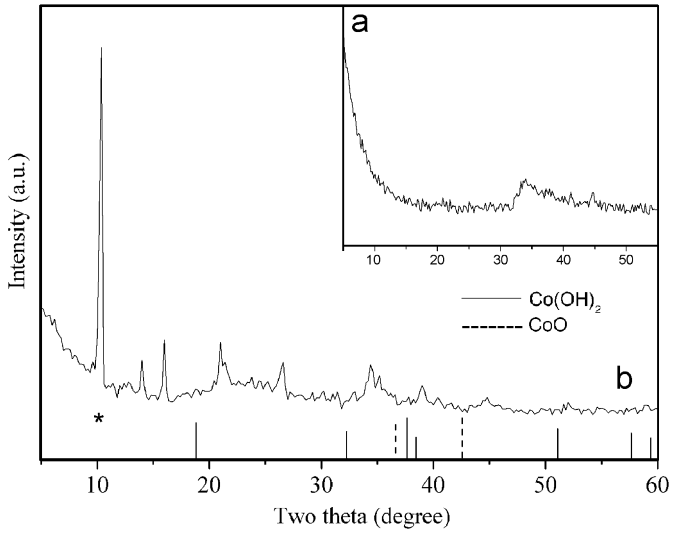

Fig. 5. The XRD pattern of the intermediate precipitate obtained in EG (a) without [OH^-], and (b) with [OH^-] (*-main peak of cobalt alkoxide (Ref. [22])).

[24], the XRD peaks varies depending on the disorder and type of polyol. It should be also noted that neither cobalt oxide nor hydroxide are formed, when cobalt acetate is used even in the presence of large concentration of [OH^-]. The FTIR spectra of (a) EG, pink colored intermediate precipitate formed in EG (b) without OH^- ions at 200 °C/15 min and precipitates formed at (c) 180 °C and (d) 190 °C in the presence of OH^- ions using cobalt acetate are shown in Fig. 6. The OH stretching at 3300 cm^{-1}, C–H stretching vibrations around 2850–2950 cm^{-1} and absorption in the fingerprint region around 1500–700 cm^{-1} are present in all the samples which indicates the presence of EG. On the other hand, the absence of the C = O stretching vibration characteristics of acetate in the range of 2000–1650 cm^{-1} and the presence of C–O vibrations in the 1000–1200 cm^{-1}

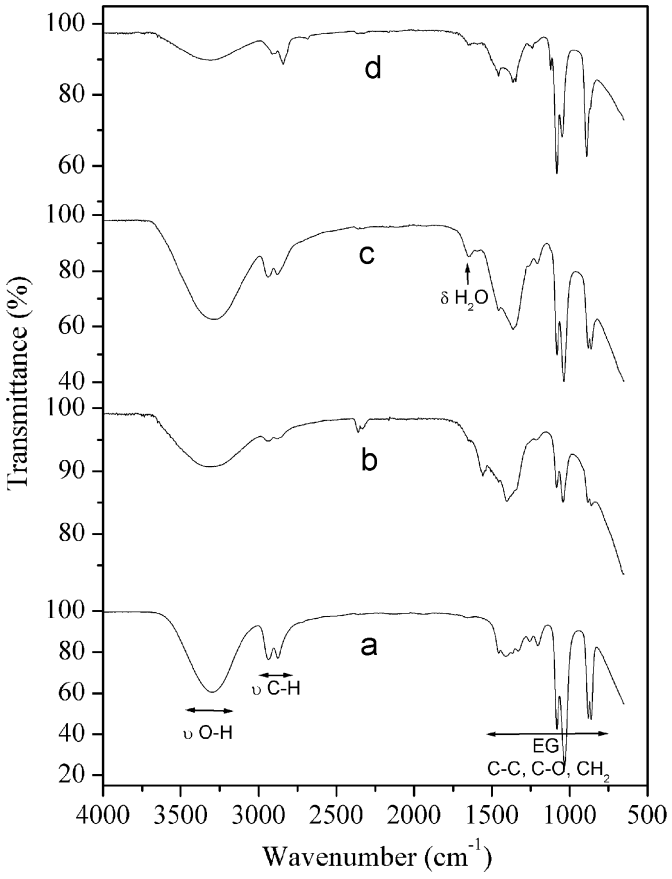

Fig. 6. The FTIR spectrum of (a) ethylene glycol, precipitate obtained in EG at (b) without [OH^-] at 200 °C, and with [OH^-] at (c) 180 °C, and (d) 190 °C.

range suggest the formation of cobalt alkoxide. Since the formation of Co complexes at milder condition is promoted by the [OH^-] ions, the morphology of these intermediate solids may also be influenced leading to variation in the reduction rate as well as the properties of metal particles. Thus, we studied the morphology of the pink colored precipitate formed after the complex formation step, prior to getting reduced to Co. The SEM micrographs of the pink colored intermediate precipitate formed in EG without [OH^-] ions at (a) 200 °C/15 min and (b) 200 °C/40 min and with [OH^-] ions at (c) 180, (d) 190 °C, (e) cobalt particles formed at 195 °C and their corresponding (f) particle size distribution are shown in Fig. 7. The sub-micron sized intermediate precipitate obtained in the absence of [OH^-] ions is spherical in shape (Fig. 7(a)) and converted to spherical Co particles after a reaction time of 40 min. The SEM micrograph of the intermediate precipitate at 200 °C/ 40 min (Fig. 7(b)) showed the presence of both cobalt alkoxide and cobalt particles. However, the cobalt alkoxide particles are hollow in nature, which is responsible for the broad peaks in the XRD pattern in Fig. 5(a). FTIR showed the presence of EG which is encased inside the hollow sphere. The alkoxide formed at 180 °C in the presence of [OH^-] ions are composed of nanometer-sized particles (Fig. 7(c)) and undergoes dissolution (Fig. 7(d)) before getting reduced to form Co particles at 195 °C (Fig. 7(e)) with an average size of 75 nm as shown in the particle size distribution plot (Fig. 7(f)). A mixture of cobalt alkoxide and cobalt are observed in the dissolution stage and finally only Co particles are observed at the end of the reaction. Although the cobalt alkoxide particles observed in SEM showed submicron sized hollow particles, detailed TEM observation revealed that they are amorphous. Also, inorder to ascertain the crystallinity of the samples, selected area diffraction (SAED) patterns were recorded for the cobalt alkoxide, the solid present during the dissolution stage and the final cobalt particles which are shown in Figs. 8(a)–(c), respectively. It is clearly observed that the cobalt alkoxide is amorphous as seen from the diffused SAED pattern (Fig. 8a) that is in accordance with the XRD results. The SAED pattern of the samples taken during the dissolution stage indicated the slight appearance of diffuse ring pattern which indicated that the samples are in the process of crystallization (Fig. 8(b)) and finally the cobalt particles showed dotted pattern indicating their crystalline nature (Fig. 8(c)). Also, the influence of hydroxyl ions is clear as the dissolution and formation of Co particles at boiling point of EG are reduced immediately in the presence of [OH^-] ions whereas it takes nearly an hour in the absence of [OH^-] ions. These results suggest that the rate-determining step is the metal complex forming reaction, which is influenced very much by the [OH^-] ion concentration. The above results also justify that the cobalt alkoxides are converted to Co metal and the reaction is accelerated in the presence of [OH^-] ions. The reduction of Co from cobalt alkoxide also suggests that the Eq. (1) can be extended to alkoxides also (Eq. (3)).

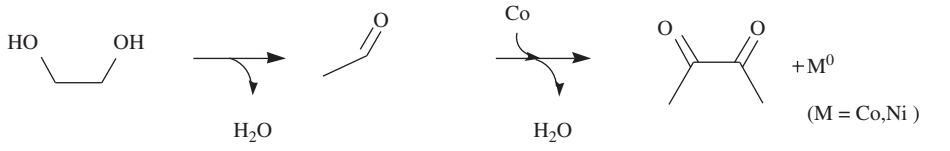

(3)

In contrast to the experiments with cobalt acetate in which the reduction rate is enhanced with [OH^-] ions, cobalt chloride could not be reduced within the observed

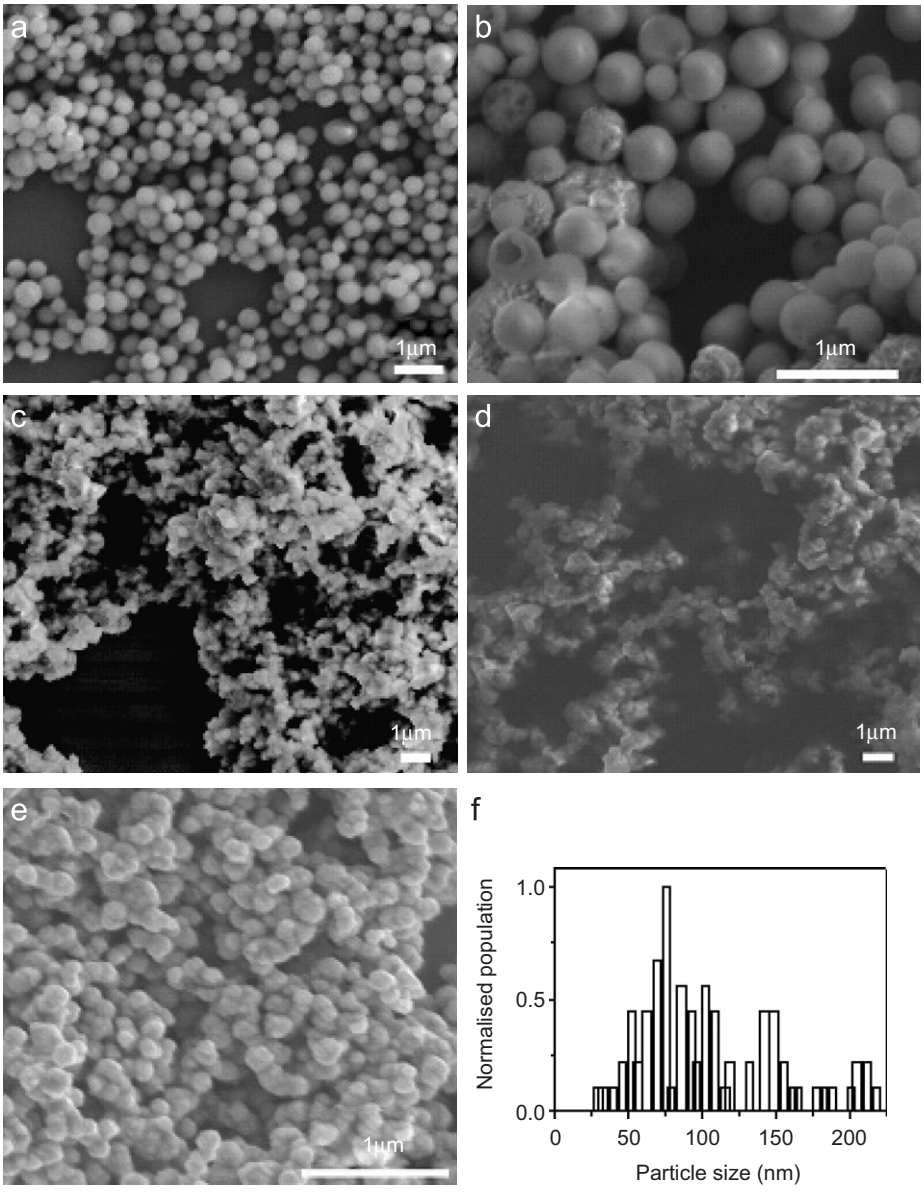

Fig. 7. The SEM micrographs of the intermediate precipitates obtained in EG without [OH^-] at (a) 200 °C/15 min, (b) 200 °C/40 min, with [OH^-] at (c) 180 °C, (d) 190 °C, (e) cobalt particles at 195 °C and their corresponding (f) particle size distribution plot.

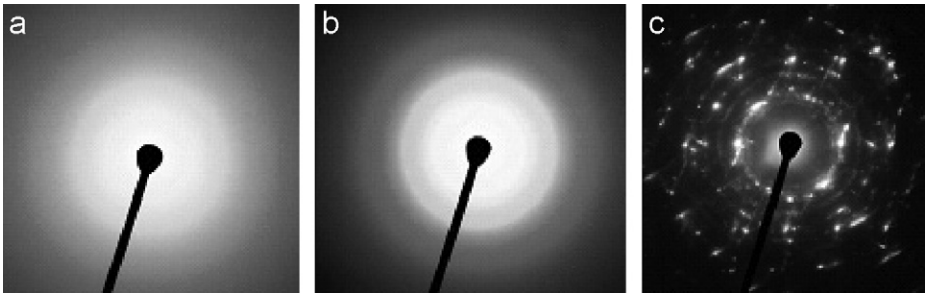

Fig. 8. The SAED pattern of (a) cobalt alkoxide (b) solids at the dissolution stage and (c) cobalt particles.

experimental duration even with [OH^-] ions. Though the oxidation reaction of EG is enhanced with the addition of [OH^-], the complex formed in the case of cobalt chloride is not in the reducible form for the reaction leading to the formation of cobalt metal to progress. On the other hand when cobalt hydroxide is used as precursor, cobalt metal is

formed without going through the formation of any other intermediates that was confirmed by monitoring the products at various time intervals. This could easily be understood by comparing Eqs. (1) and (3). According to Eq. (1), the oxidation product of diacetyl forms with hydroxides, whereas in Eq. (3) cobalt alkoxide is reduced. Thus, in the case of cobalt hydroxide, it dissolves to form cobalt ion that has a standard reduction potential value within the reducible limits of polyols as shown in Fig. 3.

3.3. Effect of polyols

Since the reduction using polyol process is reported to be slow, in most cases the synthesis of cobalt nanoparticles of smaller size are achieved by either using surfactants [42] or using heterogeneous nucleation agents such as Pt or Pd [43]. However, the reaction kinetics can be enhanced by proper choice of polyols. Since the experimental evaluation of the oxidation/reduction potential of polyol at boiling point was difficult, molecular orbital calculations were carried out to determine the reduction potential of polyol [44]. Here, the direction of electron transfer (polyol to metal or metal to polyol) and the relative levels of highest occupied molecular orbital (HOMO) and lowest unoccupied molecular orbital (LUMO) of polyol and metal were considered. Then, to estimate the reduction potential, either the metal or the polyol parameters should be fixed. Here, we fixed the metal salts singly occupied molecular orbital (SOMO) and considered different types of polyol.HOMO energy levels suggested that EG has lower value (−9.111 eV) compared to TMEG (−8.903 eV) as illustrated in Fig. 9. A higher value for HOMO signifies the ability of the polyol to donate electrons. Also, the reaction rate could be further enhanced with the introduction of [OH^-] as discussed earlier. The complex forming reactions occur at milder reaction condition such as low temperature and [OH^-] concentration and lesser reaction duration in TMEG than in EG. In order to qualitatively evaluate the reaction rate of polyol, we compared the UV–visible spectrum of cobalt acetate in EG and TMEG in the presence of [OH^-] ions. Fig. 10 shows the UV–visible spectra of Co-EG-[OH^-] and Co-TMEG-[OH^-] systems at 150 °C. In contrast to the absorption peaks at 575, 520 and 462 nm corresponding to various metal complexes in Co-EG-[OH^-] system, the reaction in Co-TMEG-[OH^-] system progresses very rapidly and forms the pink intermediate precipitate. Consequently, the absorption peaks corresponding to cobalt complexes were not detected. The FTIR spectrum of TMEG and the pink colored precipitate obtained in TMEG are shown in Figs. 11 (a) and (b), respectively. The C-H vibration near 2850 cm^{-1} is split. The strong absorption in the 1000–1200 cm^{-1} range corresponds to C–O stretching type. However, the OH stretching vibration in the range of 3200–3650 cm^{-1} and C = O in the range of 2000–1650 cm^{-1} were absent. The presence of C–O vibration and the absence of O–H and C = O suggests that the precipitate obtained in TMEG is cobalt alkoxide. Furthermore, the XRD of the intermediate precipitates obtained in TMEG with and without [OH^-] ions as shown in Figs. 12(a) and (b) respectively are in agreement with the main peaks of cobalt alkoxide [22]. The grain size of the cobalt alkoxide formed with [OH^-] ions in TMEG showed only a few tens of nm and the intensities of the diffraction peaks at higher angles were low and were not observed clearly. The morphology of the nanometer ranged alkoxide precipitate formed in the presence of [OH^-] ion in TMEG is very small as shown in Fig. 13 than the ones obtained in EG (Fig. 7(c)). The decrease in alkoxide particle size is believed to determine the rate of metal forming reactions. The diameter of the cobalt metal particles was comparatively smaller in TMEG-[OH^-] (Fig. 14a) with an average particle size of 60 nm (Fig. 14b) than the ones obtained in EG-[OH^-] system whose average particle size is 75 nm. The decrease in the size of the cobalt nanoparticles is due to the faster reaction kinetics. Slow reaction kinetics would result in the decrease in the concentration of the ions for reduction and would end up in making larger particles. Moreover, the enhanced reaction kinetics of TMEG-[OH^-] system compared to EG-[OH^-] can be utilized to obtain metastable structures such as hcp-Co and Ni from our previous studies [43,45]. These studies suggest that the complex forming reaction is the rate-determining step of the polyol process. The metal complex that facilitates the formation of the intermediates such as metal alkoxide, which is reduced to form the metal particles, determines the rate of the entire process. Finally it can be shown that the overall reaction in the reduction of Co proceeds as follows:

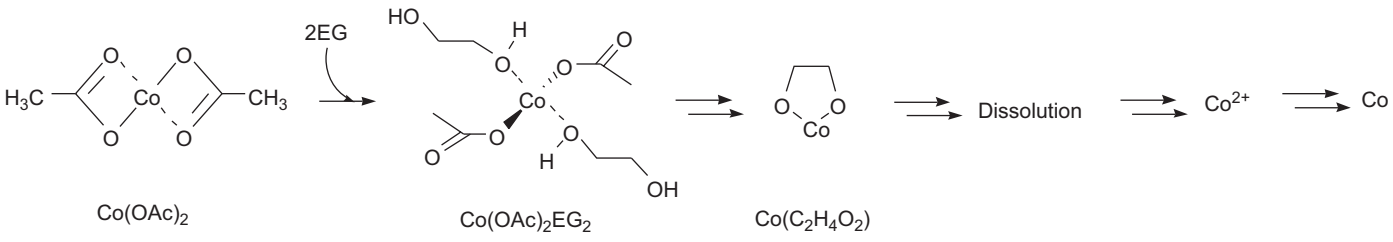

(4)

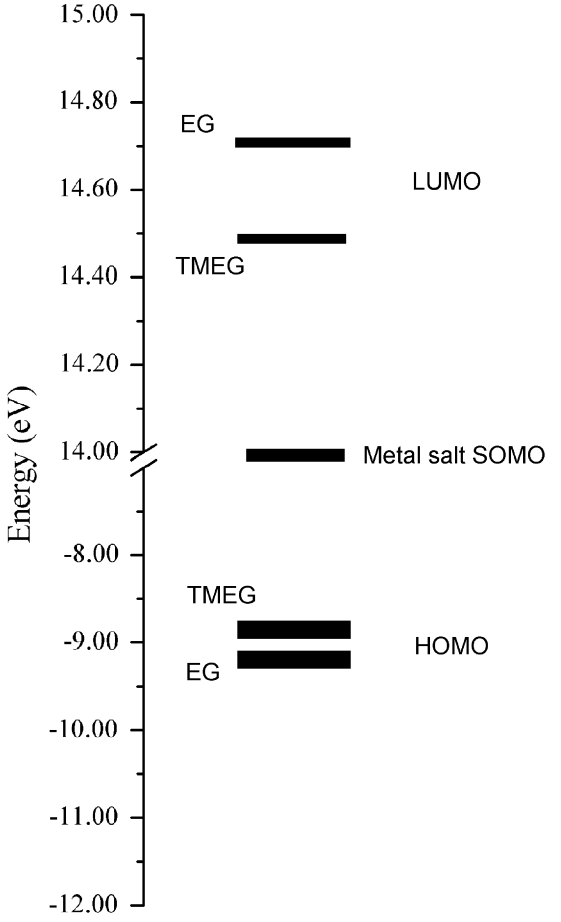

Fig. 9. The HOMO and LUMO energy levels for TMEG and EG on comparison with SOMO for metal salts.

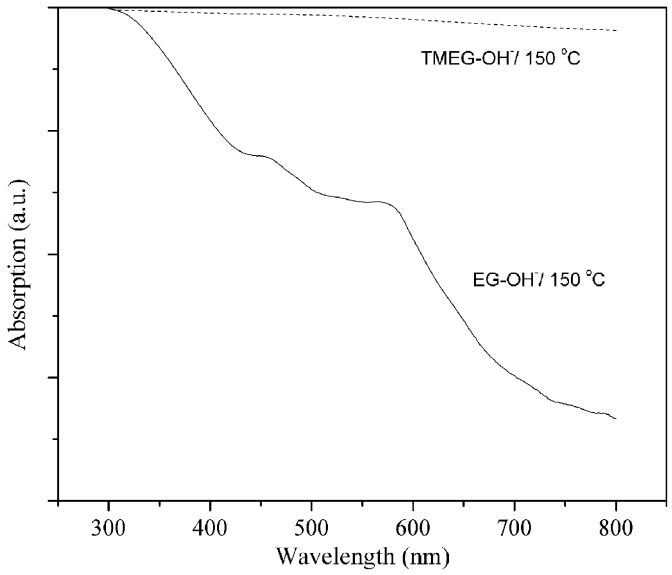

Fig. 10. The UV–visible spectra of Co-EG-[OH^-] and Co-TMEG-[OH^-] systems at 150 °C.

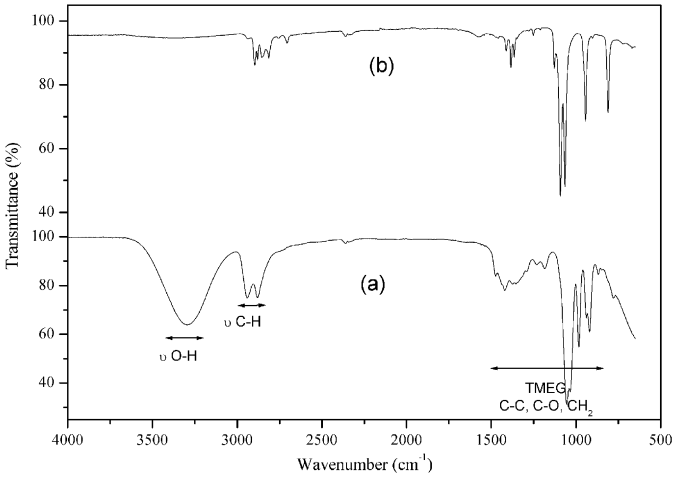

Fig. 11. The FTIR spectrum of (a) TMEG, and (b) intermediate precipitate obtained in TMEG at 200 °C.

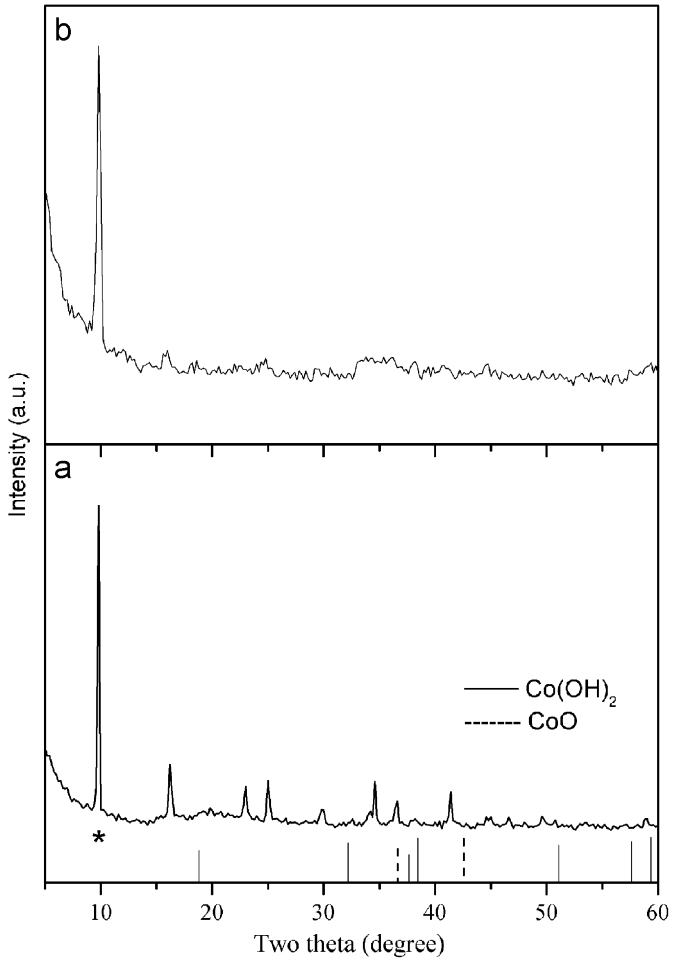

Fig. 12. The XRD pattern of the intermediate precipitates obtained in TMEG (a) without [OH^-], and (b) with [OH^-]. (*—main peak of cobalt alkoxide (Ref. [22])).

3.4. Synthesis of alloys using polyol process

Although the synthesis of metals is found to be straightforward, the synthesis of transition metal alloys in polyols is difficult, as both the metals should be co-reduced to obtain their corresponding alloys. The synthesis of noble metal based alloys are easier to achieve compared to

transition metal alloys since the standard reduction potential of noble metals are higher as shown in Fig. 3. Hence the catalytic property of the noble metals also helps in the formation of alloys such as FePt, MnPt, CoPt, etc. [3,46–48]. However, to obtain a transition metal alloy such as FeCo, the coreduction of Fe and Co should be realized at the same temperature. Fe could be reduced at 120 °C using $FeCl_2$ and NaOH in EG. But the proper choice of cobalt precursor is essential to reduce at lower temperature along with Fe.

From this study, it could be said that this can be realized by using cobalt acetate rather than $CoCl_2$, which does not form a reducible complex at low temperatures. Even using cobalt acetate, the reaction rate has to be enhanced to accommodate the reduction of the same at low temperatures. Although the use of TMEG instead of EG would enhance the reaction rate further, it would also influence the reduction of both Co and Fe and would not help to reduce the gap any further. Hence the control over the reaction temperature, which does not influence the reduction rate of Fe above 120 °C considerably on one hand, and influences the reduction of Co ion on the other, was used to facilitate the coreduction of Co and Fe. EG-[OH^-] system is found to be a better choice resulting in FeCo alloys of various sizes and composition [49]. Similarly the co-reduction of FePt at low temperatures is also achieved by the control of the reaction kinetics. By using chloride precursor of Fe and [OH^-] as additive, the reaction rate could be enhanced [50] to obtain FePt even at 120 °C against the ones achieved at higher temperature using acetates and acetylacetonates [51], and making use of the catalytic action of Pt. To summarize, we propose that the synthesis of metal or alloy particles can be designed by monitoring the complex forming reaction by studying the effect of precursors, additives such as [OH^-] ions, polyols, etc. This has paved the way for the synthesis of composition and size controlled alloys and will pave the way for new functional materials using polyol process in the near future.

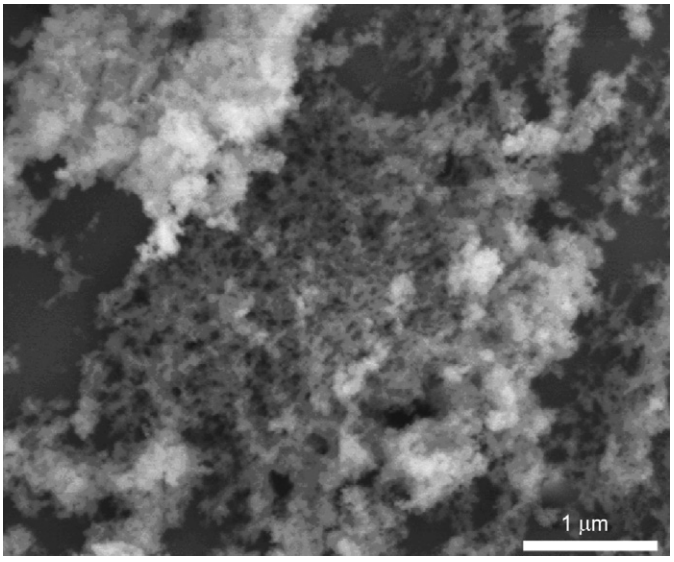

Fig. 13. The intermediate cobalt alkoxide obtained in TMEG in the presence of [OH^-].

4. Conclusion

The rate-determining step of the polyol process was investigated using Co-polyol-[OH^-] system. The metal salts dissolved in polyol were found to undergo the formation of metal complex, metal alkoxide and finally the reduction reaction depending on the type of precursors. The metal complex forming reaction was found to determine the physical properties of the final product. The reaction rate is enhanced in the presence of [OH^-] ions by accelerating the oxidation reaction of polyol. The above can also be further enhanced by selecting a highly reducing polyol. Co ions are found to reduce to Co metal from either cobalt alkoxide or cobalt hydroxide by dissolution. These studies provided the necessary insight of polyol process and lead to the successful synthesis of metal (Fe) and alloys (FeCo) that were not realized in the past.

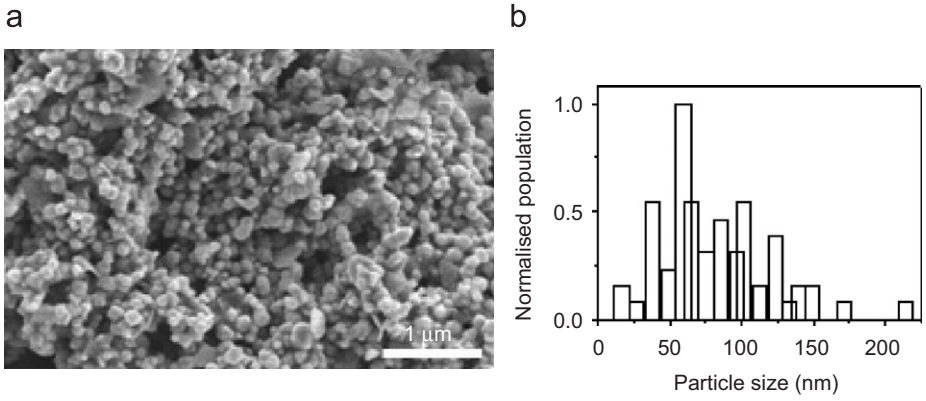

Fig. 14. (a) The SEM micrograph of the Co particles synthesized in TMEG in the presence of [OH^-] and their corresponding (b) particle size distribution plot.

Acknowledgments

This work was supported by Grant-in-Aid for Basic Research #(A) 17201021 and #(S) 14103016 from the Ministry of Education, Science, Culture and Sport of Japan, and Grant-in-Aid # 0171078-A from the Iketani Science and Technology Foundation. We thank K. Motomiya for the TEM measurements.

Appendix A. Supplementary data

Supplementary data associated with this article can be found in the online version at doi:10.1016/j.jssc.2007.07.024.

References

[1] F. Fievet, J.P. Lagier, B. Blin, B. Beaudoin, M. Figlarz, Solid State Ionics 32-3 (1989) 198.
[2] L.K. Kurihara, G.M. Chow, P.E. Schoen, Nanostruct. Mater. 5 (1995) 607.
[3] B. Jeyadevan, K. Urakawa, A. Hobo, N. Chinnasamy, K. Shinoda, K. Tohji, D.D.J. Djayaprawira, M. Tsunoda, M. Takahashi, Jpn. J. Appl. Phys. 42 (2003) L350.
[4] P.Y. Silvert, R. Herreraurbina, K. Tekaiaelhsissen, J. Mater. Chem. 7 (1997) 293.
[5] P.Y. Silvert, K. Tekaiaelhsissen, Solid State Ionics 82 (1995) 53.
[6] T. Herricks, J.Y. Chen, Y.N. Xia, Nano Lett. 4 (2004) 2367.
[7] A.K. Sra, T.D. Ewers, R.E. Schaak, Chem. Mater. 17 (2005) 758.
[8] F. Fievet, F. Fievet-Vincent, J.P. Lagier, B. Dumont, M. Figlarz, J. Mater. Chem. 3 (1993) 627.
[9] G. Viau, F. Fievet-Vincent, F. Fievet, Solid State Ionics 84 (1996) 259.
[10] R.E. Cable, R.E. Schaak, Chem. Mater. 17 (2005) 6835.
[11] P.Y. Silvert, R.H. Urbina, N. Duvauchelle, V. Vijayakrishnan, K.T. Elhsissen, J. Mater. Chem. 6 (1996) 573.
[12] Y.G. Sun, Y.N. Xia, Science 298 (2002) 2176.
[13] T. Hinotsu, B. Jeyadevan, C.N. Chinnasamy, K. Shinoda, K. Tohji, J. Appl. Phys. 95 (2004) 7477.
[14] S.-H. Wu, D.-H. Chen, J. Colloid Inter. Sci. 259 (2003) 282.
[15] M.S. Hegde, D. Larcher, L. Dupont, B. Beaudoin, K. Tekaia-Elhsissen, J.-M. Tarascon, Solid State Ionics 93 (1997) 33.
[16] N. Chakroune, G. Viau, C. Ricolleau, F. Fievet-Vincent, F. Fievet, J. Mater. Chem. 13 (2003) 312.
[17] G. Viau, F.F. Vincent, F. Fievet, J. Mater. Chem. 6 (1996) 1047.
[18] R.J. Joseyphus, D. Kodama, T. Matsumoto, Y. Sato, B. Jeyadevan, K. Tohji, J. Magn. Magn. Mater. 310 (2007) 2393.
[19] L.-S. Zhong, J.-S. Hu, H.-P. Liang, A.-M. Cao, W.-G. Song, L.-J. Wan, Adv. Mater. 18 (2006) 2426.
[20] D. Larcher, R. Patrice, J. Solid State Chem. 154 (2000) 405.
[21] L. Paul, N. Jouini, F. Fievet, Chem. Mater. 12 (2000) 3123.
[22] D. Larcher, G. Sudant, R. Patrice, J.M. Tarascon, Chem. Mater. 15 (2003) 3543.
[23] L. Poul, S. Ammar, N. Jouini, F. Fievet, J. Sol-Gel Sci. Technol. 26 (2003) 261.
[24] N. Chakroune, G. Viau, S. Ammar, N. Jouini, P. Gredin, M.J. Vaulay, F. Fievet, New J. Chem. 29 (2005) 355.
[25] D.I.G. Gutierrez, C.E.G. Wing, L. Giovanetti, J.M.R. Lopez, F.G. Requejo, M.J. Yacaman, J. Phys. Chem. B 109 (2005) 3813.
[26] G. Carotenuto, G.P. Pepe, L. Nicolais, Eur. Phys. J. B 16 (2000) 11.
[27] M. J. Frisch, et al., Gaussian 98, Revision A.9, Gaussian, Inc., Pittsburgh PA, 1998.
[28] [a] W.J. Hehre, R.F. Stewart, J.A. Pople, J. Chem. Phys. 51 (1969) 2657;
[b] J.B. Collins, P.V.R. Schleyer, J.S. Binkley, J.A. Pople, J. Chem. Soc. 64 (1976) 142;
[c] P.J. Hay, W.R. Wadt, J. Chem. Phys. 82 (1985) 270;
[d] W.R. WadtP. J. Hay, J. Chem. Phys. 82 (1985) 284;
[e] P.J. Hay, W.R. Wadt, J. Chem. Phys. 82 (1985) 299.
[29] [a] R. Seeger, J.A. Pople, J. Chem. Phys. 66 (1977) 3045;
[b] R. Bauernschmitt, R. Ahlrichs, J. Chem. Phys. 104 (1996) 9047;
[c] P. Carsky, I. Hubak, Theo. Chim. Acta 80 (1991) 407.
[30] B. Jeyadevan, K. Shinoda, R.J. Justin, T. Matsumoto, K. Sato, H. Takahasi, Y. Sato, K. Tohji, IEEE Trans. Magn. 42 (2006) 3030.
[31] A.B.P. Lever, Inorganic Electronic Spectroscopy, Elsevier, Amsterdam, 1968.
[32] L.I. Katzin, E. Gebert, J. Chem. Phys. 72 (1950) 5464.
[33] B. Blin, F. Fievet, D. Beaupere, M. Figlarz, New. J. Chem. 13 (1989) 67.
[34] C.F.H. Allen, J. Chem. Soc. 52 (1930) 2955.
[35] R.C. Lawrence, Nature 205 (1965) 1313.
[36] M.F. Pool, A.A. Klose, J. Am. Oil Chem. Soc. (1951) 215.
[37] K. Fung, D. Grosjean, Anal. Chem. 53 (1981) 168.
[38] G. Milazzo, S. Caroli, Tables of Standard Electrode Potentials, Wiley, Newyork, 1978.
[39] D. Dobos, Electrochemical Data, Elsevier, Amsterdam, 1975.
[40] F. Bonet, C. Guery, D. Guyomard, R.H. Urbina, K. Tekaia-Elhsissen, J.-M. Tarascon, Int. J. Inorg. Mater. 1 (1999) 47.
[41] A. Henglein, M. Giersig, J. Phys. Chem. B 104 (2000) 6767.
[42] S.I. Cha, C.B. Mo, K.T. Kim, S.H. Hong, J. Mater. Res. 20 (2005) 2148.
[43] O. Perales-Perez, B. Jeyadevan, C. N. Chinnasamy, K. Tohji, A. Kasuya, In Inorganic Materials: Recent Advances, (Eds.), D. Bahadur, S. Vitta, O. Prakash, Narosha, Publishing House, New Delhi, India, 2004, p. 9.
[44] T. Matsumoto et al. (unpublished).
[45] C.N. Chinnasamy, B. Jeyadevan, K. Shinoda, K. Tohji, A. Narayanasamy, K. Sato, S. Hisano, J. Appl. Phys. 97 (2005) 10J309.
[46] D.C. Lee, A. Ghezelbash, C.A. Stowell, B.A. Korgel, J. Phys. Chem. B 110 (2006) 20906.
[47] C.N. Chinnasamy, B. Jeyadevan, K. Shinoda, K. Tohji, J. Appl. Phys. 93 (2003) 7583.
[48] Y. Vasquez, K.A. Sra, R.E. Schaak, J. Am. Chem. Soc. 127 (2005) 12504.
[49] D. Kodama, K. Shinoda, K. Sato, Y. Konno, R.J. Joseyphus, K. Motomiya, H. Takahashi, T. Matsumoto, Y. Sato, K. Tohji, B. Jeyadevan, Adv. Mater. 18 (2006) 3154.
[50] R.J. Joseyphus, B. Jeyadevan, K. Shinoda, Y. Sato, K. Tohji, J. Mater. Sci., in press.
[51] L.C. Varanda, M. Jafelicci Jr., J. Am. Chem. Soc. 128 (2006) 11062.